A&A 462, 1187–1198 (2007)
DOI: 10.1051/0004-6361:20065881

Astronomy & Astrophysics

Effects of CO_2 on H_2O band profiles and band strengths in mixed H_2O:CO_2 ices

K. I. Öberg[1], H. J. Fraser[2], A. C. A. Boogert[3], S. E. Bisschop[1], G. W. Fuchs[1], E. F. van Dishoeck[4], and H. Linnartz[1]

[1] Sackler Laboratory for Astrophysics, Leiden Observatory, University of Leiden, PO Box 9513, 2300 RA Leiden, The Netherlands
e-mail: oberg@strw.leidenuniv.nl
[2] Department of Physics, Scottish Universities Physics Alliance (SUPA), University of Strathclyde, John Anderson Building, 107 Rottenrow East, Glasgow G4 ONG, Scotland
[3] AURA/NOAO-South, Casilla 603, La Serena, S. A. Chile
[4] Leiden Observatory, University of Leiden, PO Box 9513, 2300 RA Leiden, The Netherlands

Received 22 June 2006 / Accepted 17 October 2006

ABSTRACT

Context. H_2O is the most abundant component of astrophysical ices. In most lines of sight it is not possible to fit both the H_2O 3 μm stretching, the 6 μm bending intensities with a single pure H_2O spectrum. Recent Spitzer observations have revealed CO_2 ice in high abundances and it has been suggested that CO_2 mixed into H_2O ice can affect the positions, shapes and relative strengths of the 3 μm and 6 μm bands.
Aims. We investigate whether the discrepancy in intensity between H_2O bands in interstellar clouds and star forming regions can be explained by CO_2 mixed into the observed H_2O ice affecting the bands differently.
Methods. Laboratory infrared transmission spectroscopy is used to record spectra of H_2O:CO_2 ice mixtures at astrophysically relevant temperatures and composition ratios.
Results. The H_2O peak profiles and band strengths are significantly different in H_2O:CO_2 ice mixtures compared to pure H_2O ice. The ratio between the strengths of the 3 μm and 6 μm bands drops linearly with CO_2 concentration such that it is 50% lower in a 1:1 mixture compared to pure H_2O ice. In all H_2O:CO_2 mixtures, a strong free-OH stretching band appears around 2.73 μm, which can be used to put an upper limit on the CO_2 concentration in the H_2O ice. The H_2O bending mode profile also changes drastically with CO_2 concentration; the broad pure H_2O band gives way to two narrow bands as the CO_2 concentration is increased. This makes it crucial to constrain the environment of H_2O ice to enable correct assignments of other species contributing to the interstellar 6 μm absorption band. The amount of CO_2 present in the H_2O ice of B5:IRS1 is estimated by simultaneously comparing the H_2O stretching and bending regions and the CO_2 bending mode to laboratory spectra of H_2O, CO_2, H_2O:CO_2 and HCOOH.

Key words. astrochemistry – line: profiles – molecular data – methods: laboratory – ISM: molecules – infrared: ISM

1. Introduction

Infrared spectroscopy towards dense molecular clouds and young stellar objects (YSOs) often reveals prominent bands attributed to H_2O ice. The 3.08 μm (3250 cm^{-1}) band, attributed to the H_2O stretching mode, and the 6.0 μm (1700 cm^{-1}) band, attributed to the H_2O bending mode, are detected in many lines of sight (Willner et al. 1982; Tanaka et al. 1990; Murakawa et al. 2000; Boogert et al. 2000; Keane et al. 2001; Gibb et al. 2004; Knez et al. 2005). Also the observation of the H_2O libration mode at 13 μm (770 cm^{-1}) has been reported (Keane et al. 2001; Gibb et al. 2004). It is a long-standing problem in the interstellar community that the H_2O ice 6.0/3.08 band intensity ratio in astrophysical observations is up to 2 times higher than expected for pure H_2O ice (Keane et al. 2001).

This discrepancy has previously been explained by absorptions of other volatile molecules and organic refractory material absorbing around 6 μm (Schutte et al. 1996; Keane et al. 2001; Gibb & Whittet 2002). These theories were put forward to explain the strong absorption of the 6.0 μm feature as well as why its shape does not match that of pure H_2O ice very well in many lines of sight. Keane et al. (2001) identified two additional components in the H_2O 6.0 μm bending mode region, centered around 5.83 μm (1720 cm^{-1}) and 6.2 μm (1600 cm^{-1}), when subtracting a pure H_2O ice spectrum that was fitted to the 3.08 μm stretching band. Analyzing the residuals after subtracting the H_2O bending mode presupposes that the profile of the H_2O bending mode is well known. Hence knowledge of the H_2O bending mode profile in different environments is critical to correctly assign other species contributing to the 6 μm band.

Pontoppidan et al. (2005) showed that for observations of ices in circumstellar disks, part of the discrepancy in intensities between the H_2O bands may be due to disk geometry because of scattering at short wavelengths. However, since this anomaly is almost always present to some degree in disks and envelopes, as well as in clouds, it is unlikely to be the entire explanation. In the sources where the 13 μm H_2O libration band is visible, it is possible to fit the H_2O stretching and libration peaks with a single H_2O ice abundance, while fitting the 6 μm band independently results in a much higher column density (Gibb et al. 2004). The fact that the libration mode at 13 μm is in agreement with the 3 μm band refutes the idea that the excess at 6 μm is due to wavelength dependent scattering.

Recently Knez et al. (2005) suggested that the ratio in band intensity could be due to large amounts of CO_2 mixed in with the H_2O ice. Observations reveal that solid CO_2 is common in many lines of sight (Gerakines et al. 1999; Gibb et al. 2004). With the Infrared Space Observatory (ISO), the CO_2 stretching mode at

4.25 μm (2350 cm^{-1}) was observed toward Taurus background stars (Whittet et al. 1998; Nummelin et al. 2001). More recently the launch of the Spitzer Space Telescope made the CO_2 bending mode at 15 μm (670 cm^{-1}) available for observations and the band has been detected towards several background stars (Bergin et al. 2005; Knez et al. 2005). The average abundance with respect to H_2O ice towards the Taurus sources is 20%, but up to 37% has been observed (Knez et al., in prep.). Toward several protostars up to 35% of CO_2 compared to H_2O has been observed (Nummelin et al. 2001; Boogert et al. 2004), making CO_2 one of the most abundant ices after H_2O.

In a previous study, using the H_2O column density from the 3.08 μm band and laboratory spectra of pure H_2O ice, Knez et al. (2005) determined that the H_2O bending mode contributes 77% and 69% to the observed 6.0 μm absorption features towards Elias 16 and CK 2, respectively. Using a combination of laboratory spectra of two H_2O:CO_2 mixtures, 1:1 and 10:1 respectively, they showed that 85% to 100% of the 6.0 μm band strength can be explained by H_2O. This is due to the smaller ratio between the stretching and bending mode strengths seen in an unpublished H_2O:CO_2 1:1 spectrum by Ehrenfreund (private communication). This combination of spectra, together with a water-poor mixture spectrum, also fits the CO_2 profile well, with approximately 80% of the CO_2 in the water rich ice (Knez et al. 2005). Hence it is not unlikely that a significant part of the H_2O ice is in H_2O:CO_2 ice mixtures close to 1:1 in many lines of sight, even if the average abundances of H_2O and CO_2 is closer to 3:1.

The question that prompted this study is whether there is a change in H_2O band profiles and relative H_2O band strengths in ice mixtures compared to pure H_2O ice, for H_2O:CO_2 ice mixtures that are both astrophysically relevant and contain enough H_2O to observe with e.g. Spitzer. Such information in turn, is a prerequisite for determining whether additional species contribute to the 6 μm band. In this work we present a systematic study of the infrared properties of H_2O absorptions in H_2O:CO_2 ice mixtures around 1:1, for the temperature range of 15 to 135 K, in order to constrain the effect that CO_2 has on the shapes and relative band strengths of the H_2O bands.

2. Previous laboratory data

Two previous studies have reported changes in the H_2O bands in H_2O:CO_2 ice mixtures compared to pure H_2O ices (Hagen et al. 1983; Schmitt et al. 1989). In both cases, only one isolated H_2O:CO_2 mixture, 1:2 and 10:1 respectively, was investigated. In both the 1:2 and 10:1 H_2O:CO_2 mixture spectra a new H_2O band appears around 2.74 μm, the relative strength of the bending mode increases and all the band profiles change compared to a pure H_2O ice spectrum. No attempts were made to quantify these changes.

A number of later laboratory studies focused on H_2O:CO_2 ice mixtures as well, but to our knowledge none of them systematically studied the impact of CO_2 on water ice and none of them has reported on changes in the H_2O band profiles and band strengths due to CO_2. This is not surprising, since most of the studies focused on mixtures with H_2O as the dominant ice component (Hudgins et al. 1993; Bernstein et al. 2005). Only a few laboratory spectra of H_2O:CO_2 mixtures close to 1:1 exist in the literature (Gerakines et al. 1995; Palumbo & Baratta 2000; Gerakines et al. 2005). The effect of CO_2 on H_2O ice features is only considered by Gerakines et al. (2005), who concluded from the spectra of a H_2O:CO_2 1.6:1 ice mixture that the relative H_2O band intensities were not affected by high concentrations of CO_2. Nevertheless, the 3.08/6.0 μm band strength ratio can be calculated from their reported integrated intensities and reveals a drop of ~30% compared to pure H_2O.

It is well known from matrix isolation experiments that the different H_2O bands have different relative band strengths dependent on H_2O cluster size (van Thiel et al. 1957). The band strength of the bending mode is much less affected by the H_2O cluster size than the stretching mode, when the H_2O cluster size is changed by varying the H_2O concentration in a N_2 matrix. The former band strength drops by 20% when the matrix to H_2O ratio is decreased by one order of magnitude while the stretching band strength increases by a factor of 10. The main intensity contribution in both bands comes from the monomer peak when the H_2O concentration is low and from a cluster mixture when the concentration is high (high concentration meaning N_2:H_2O 1:10, van Thiel et al. 1957). The position of the bending modes is approximately the same for all cluster sizes, while the major stretching mode peak shifts from 3400 cm^{-1} at high H_2O concentrations to the position of the free-OH stretch at low concentrations (~3690 cm^{-1} or ~2.7 μm). Finally, the relative band strengths are also affected by the type of matrix used, e.g. noble gas or nitrogen or oxygen. This has been reported also for H_2O in astronomically relevant matrices (Ehrenfreund et al. 1996). It is important to note that none of these matrices forms hydrogen bonds with H_2O, thus no conclusions about the band strengths and band profiles of H_2O can be drawn from these experiments concerning H_2O in a hydrogen bonding matrix. Another astrophysically relevant molecule, CO, does probably form hydrogen bonds with H_2O in amorphous ice mixtures (Schmitt et al. 1989). Matrix experiments have also shown that CO forms weak hydrogen bonds, while CO_2 does not (Tso & Lee 1985).

3. Experiment and data analysis

3.1. Experiment

All experiments were conducted in a high vacuum (HV) chamber described in detail elsewhere (Gerakines et al. 1995) at a base pressures below 1.3×10^{-6} Torr at room temperature. Ices of $C^{18}O_2$ (Praxair 97% purity) and H_2O (deionized and further purified through sequential freeze-thawing in a vacuum manifold) were grown on a CsI window, precooled to 15 K (45 K for one specific experiment), via effusive dosing at a growth rate of ~10^{16} molecules cm^{-2} s^{-1} roughly along the surface normal. $C^{18}O_2$ was used instead of the main isotopologue of CO_2 to minimize overlap between H_2O and CO_2 spectral features. Transmission Fourier transform infrared spectra of the ice systems were recorded between 4000–400 cm^{-1} (2.5–25 μm) at a spectral resolution of 2 cm^{-1} at fixed temperatures between 15 and 135 K, using a total of 256 scans. Background spectra were acquired prior to deposition for each experiment, at the same resolution and number of scans, and automatically subtracted from the recorded ice spectra.

The pure ices were grown in situ from $C^{18}O_2$ and H_2O gas bulbs that were filled to a total pressure of 10 mbar, prepared in a glass-vacuum manifold at a base-pressure of ~10^{-4} mbar. Mixed ices were made by dosing gas from premixed H_2O:$C^{18}O_2$ bulbs, also prepared in the glass-vacuum manifold.

The ice mixtures studied here are summarized in Table 1. The relative concentrations for the H_2O:$C^{18}O_2$ mixtures range from 20 to 80% CO_2, where the % are relative to the whole ice, i.e. 20% CO_2 is equivalent to a H_2O:CO_2 4:1 mixture. The H_2O ice exposure was always kept at 3000 L

Table 1. Ice mixtures studied in this work.

Composition	H_2O (L)[a]	CO_2 (L)	Total ice exposure (L)
pure H_2O	3000	0	3000
pure CO_2	0	3000	3000
H_2O:CO_2 1:0.25	3000	750	3750
H_2O:CO_2 1:0.5	3000	1500	4500
H_2O:CO_2 1:1	3000	3000	6000
H_2O:CO_2 1:2	3000	6000	9000
H_2O:CO_2 1:4	3000	12 000	15 000
H_2O:CO_2 1:1	10 000	10 000	20 000
H_2O:CO_2 1:1	1000	1000	2000

[a] 1 L (Langmuir) = 1×10^{-6} Torr s $\approx$ 1 monolayer of molecules.

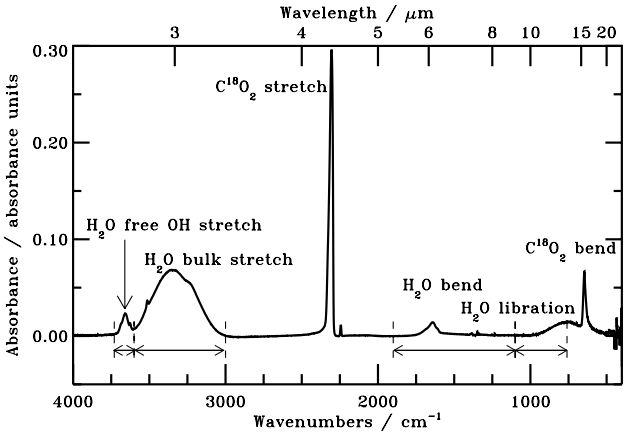

Fig. 1. Spectra over the 4000−400 cm^{-1} range of the H_2O:CO_2 1:0.5 ice mixture at 15 K. The assignments of the major peaks are indicated. The double headed arrows indicate the integration ranges for determining the intensities of the various bands; for the libration mode, only half the range is indicated (see text). Note that all CO_2 frequencies are shifted compared to those observed in space, since in the present experiments $C^{18}O_2$ has been used.

(1 L (Langmuir) = 1×10^{-6} Torr s $\approx$ 1 monolayer of molecules, assuming 10^{15} molecules cm^2 and a sticking probability of 1), except in two 1:1 control experiments with 1000 and 10 000 L H_2O exposure, respectively. The nomenclature adopted is as follows, A:B denotes a mixture with A parts of H_2O and B parts of $C^{18}O_2$.

3.2. Data analysis

The acquired spectra were first reduced to flatten the baseline by fitting a second order polynomial to the same 5 points, chosen by visual inspection well away from any features. This was done to facilitate comparison between laboratory and astronomical spectra. The curved baseline in the raw data is a real feature which is due to scattering within the ice. Flattening the spectra may hence distort profiles, but in our case no such distortion was noted. All reduced spectra can be found at `http://www.strw.leidenuniv.nl/~lab/databases/`.

Figure 1 shows an overview spectrum of a H_2O:CO_2 1:0.5 mixture. The use of the $C^{18}O_2$ isotope changes the position of the CO_2 bands compared to the main isotopologue, but does not affect the conclusions of this study. In addition to the $C^{18}O_2$ bending and stretching modes, there are two weak, narrow $C^{18}O_2$ overtone bands in the spectrum, at 3515 and 3625 cm^{-1} respectively, that overlap with the H_2O stretching bands. To calculate the integrated intensities of the H_2O bands, the H_2O peak intensities were integrated over the same wavenumber range for all spectra (see Table 2 and Fig. 1). Where narrow CO_2 peaks overlapped with the H_2O bands, a Gaussian was fitted to the CO_2 peak and subtracted from the spectrum. A Gaussian could not be fitted to the CO_2 bending mode, which overlaps with the H_2O libration mode. The band strength of the H_2O libration band was instead calculated by doubling the band strength of the high frequency half of the band. The peak frequency of the H_2O libration mode varies in the different mixtures and since the lower frequency integration bound was set to the peak frequency, the lower bound is somewhat different for different mixtures. For pure H_2O ice, this procedure was found to be accurate to within 3% compared to integrating the whole profile. To further test the induced error of this approach the band strengths were also calculated by simply subtracting the integrated area of the CO_2 bending mode from the total integrated area. The difference was less than 5%. The large interval required for the H_2O bending mode is due to its substantial low frequency wing attributed to the librational overtone (Devlin et al. 2001), which in some spectra contains more than 50% of the integrated peak intensity. The 2.73 μm band is due to free-OH stretches and its assignment to H_2O monomers, dimers and small multimers is justified in the discussion part of this paper.

Table 2. The measured peak positions and the integration bounds in cm^{-1} (μm) used to compute the integrated intensities of the H_2O peaks.

		Integration bounds	
H_2O bands	Peak	Lower	Upper
libration	780 (12.8)	500 (20.0)	1100 (9.09)[a]
bend	1655 (6.04)	1100 (9.09)	1900 (5.26)
bulk stretch	3279 (3.05)	3000 (3.33)	3600 (2.78)
free OH stretch	3661 (2.73)	3600 (2.78)	3730 (2.68)

[a] The CO_2 bending mode is excluded by explicitly taking into account only half of the libration mode profile (see text).

The substantial change in the H_2O band intensities between different mixtures reported here, prevents an independent check of the relative amount of H_2O deposited onto the surface. From three repeated experiments (of the 2:1 mixture) the standard deviations of the integrated H_2O peak intensities are estimated to be less than 10%. These experiments were carried out in the beginning and at the end of an experimental series and for separately prepared mixtures. The standard deviation hence contains the error from mixing, absolute ice exposure, measuring errors and changes in the experiment over time. Additional errors may arise from the flattening of the spectra; the difference between integrated intensities for the raw and reduced spectra is the largest for the 6.0 μm H_2O band at low H_2O concentrations; up to 40% for the 1:4 mixture. For the astrophysically relevant mixtures this uncertainty is only 1−5%, however. Some systematic errors due to the mixing procedure cannot be excluded, but are difficult to quantify. Taking all error sources into account, we estimate that the relative band strengths are accurate within ~10% for the astrophysically relevant ice mixtures, i.e. ice mixtures with less or equal amounts of CO_2 compared to H_2O.

The band strengths, A, of the three H_2O bands present in pure H_2O ice were estimated for all mixtures using the measured band strengths for pure H_2O ice at 14 K by Gerakines et al. (1995). The band strengths for the pure H_2O bands were thus set to 2.0×10^{-16} for the H_2O stretching mode, 1.2×10^{-17} for the bending mode and 3.1×10^{-17} cm $molecule^{-1}$ for the libration

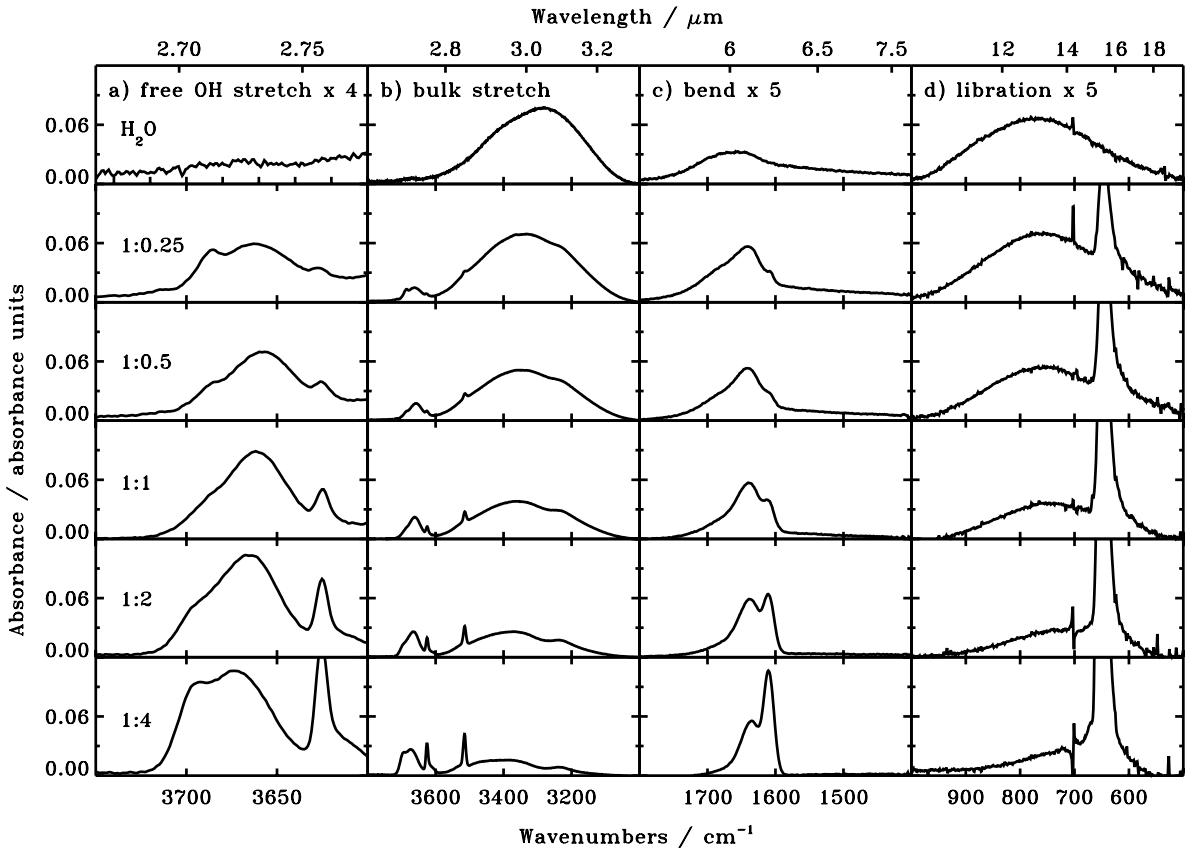

Fig. 2. Spectra over the 4000−400 cm^{-1} range at 15 K of the four H_2O peaks in H_2O:CO_2 1:x ice mixtures for different CO_2 concentrations. Each column contains one of the H_2O modes and each row one of the H_2O:CO_2 mixtures: **a)** an expanded view of the H_2O free OH stretch, **b)** the H_2O bulk and free-OH stretch, **c)** the H_2O bend and **d)** H_2O libration. The intensities of the libration, bend and free-OH stretch bands have been scaled, with a scaling factor indicated in the first row. The H_2O exposure was kept constant in all experiments. The narrow peaks around 3500 and 3630 cm^{-1} have been previously assigned to CO_2 combination modes (Sandford & Allamandola 1990). The sharp feature around 700 cm^{-1} is an experimental artifact.

band. The band strengths of these bands in the H_2O:CO_2 mixtures were calculated by scaling each integrated intensity by the band strength of the pure H_2O ice band over the pure H_2O band integrated intensity:

$$A^{\rm band}_{\rm H_2O:CO_2=1:x} = \int_{\rm band} I_{\rm H_2O:CO_2=1:x} \times \frac{A^{\rm band}_{\rm H_2O}}{\int_{\rm band} I_{\rm H_2O}} \quad (1)$$

where $A^{\rm band}_{\rm H_2O:CO_2=1:x}$ is the calculated strength of each H_2O band in the 1:x H_2O:CO_2 mixture, $\int_{\rm band} I_{\rm H_2O:CO_2=1:x}$ the measured integrated intensity of the same band, $A^{\rm band}_{\rm H_2O}$ the known strength of the pure H_2O band and $\int_{\rm band} I_{\rm H_2O}$ the integrated intensity of the pure H_2O band. The band strengths of the free OH stretch in the different mixtures were scaled to the band strength of the bulk stretching mode in pure H_2O ice. The ratios of our measured integrated intensities for pure H_2O at 15 K coincided with those of Gerakines et al. within 10%.

The calculated strengths of all H_2O bands were plotted as a function of CO_2 concentration in the ice mixture and fitted by linear models as described in detail in Sect. 4.1. These models are more accurate in predicting the band strengths for H_2O in a certain mixture than individual measurements, since they are derived from all experiments and hence the random errors are averaged out. Our model predictions agreed well with previously published isolated measurements. A spectrum by Schutte (Leiden Molecular Database) of H_2O:CO_2 1:1.25 has a stretching to bending peak ratio which lies within 5% of the value predicted by our model fit. In addition, the ratio of stretching to bending modes in the H_2O:CO_2 1.6:1 mixture from Gerakines et al. (2005) lies within 8% of our model value, further corroborating the results presented in this paper.

4. Results

4.1. Changes in H_2O band strengths and profiles with mixture composition

Figure 2 shows that the H_2O spectra at 15 K undergo two significant changes as the amount of CO_2 is increased from 0 to 80%; the profiles of the H_2O bending and stretching bands change dramatically and all H_2O integrated peak intensities change systematically with varying CO_2 concentration.

Of all modes, the profile the H_2O bending mode is most affected by the CO_2. In pure H_2O the bending mode consists of a broad peak centered at 1661 cm^{-1} (6.02 μm). The bending mode overlaps with the librational overtone, which shows up in the spectra as a low-frequency wing. To simplify comparison with astronomical observations, the wing is generally treated as a part of the bending mode when calculating band strengths. The band strength of the pure bending mode is smaller for the mixtures that have strong librational modes and hence strong librational overtones. In the spectrum of the 1:4 mixture, two narrow peaks are observed in the H_2O bending region at 1609 and 1634 cm^{-1}, instead of the broad peak and wing in the pure H_2O spectrum. The profiles of the bending mode in the other mixtures appear

Table 3. The defining parameters – peak position, *FWHM* (full width at half maximum) and peak height – of the fitted Gaussian components of the H_2O bending mode. In addition, the integrated area for each peak and their total sum are listed. The area of the libration overtone wing is also listed, but not included in the total area.

Ice mixture	Peak position [cm^{-1} (μm)]	*FWHM* [cm^{-1} (μm)]	Relative peak height	Relative integrated area	Total integrated area excl. wing
Pure H_2O	1661 (6.02)	130 (0.49)	1	1	1
	wing			0.54	
H_2O:CO_2 1:0.25	1609 (6.22)	15 (0.059)	0.056	0.0067	1.29
	1642 (6.09)	49 (0.19)	0.93	0.31	
	1661(6.02)	130 (0.49)	0.91	0.91	
	1685 (5.93)	35 (0.12)	0.22	0.055	
	wing			0.60	
H_2O:CO_2 1:0.5	1609 (6.22)	15 (0.059)	0.14	0.017	1.09
	1642 (6.09)	49 (0.19)	1.1	0.36	
	1661(6.02)	130 (0.49)	0.65	0.65	
	1685 (5.93)	35 (0.12)	0.22	0.055	
	wing			0.32	
H_2O:CO_2 1:1	1609 (6.22)	15 (0.059)	0.42	0.050	0.96
	1638 (6.11)	49 (0.19)	1.4	0.47	
	1661(6.02)	130 (0.49)	0.40	0.42	
	1685 (5.93)	35 (0.12)	0.22	0.055	
	wing			0.07	
H_2O:CO_2 1:2	1609 (6.22)	15 (0.059)	1.3	0.15	0.99
	1636 (6.11)	49 (0.19)	1.6	0.54	
	1661(6.02)	130 (0.49)	0.27	0.27	
	1685 (5.93)	35 (0.12)	0.14	0.034	
	wing			0.02	
H_2O:CO_2 1:4	1609 (6.22)	15 (0.059)	2.8	0.34	0.94
	1634 (6.12)	49 (0.19)	1.7	0.57	
	1685 (5.93)	35 (0.12)	0.14	0.034	
	wing			0.01	

to be a composition of the peaks in the pure H_2O spectra and the H_2O:CO_2 1:4 mixture. To test this, Gaussian profiles were fitted to the bending peak of the pure H_2O ice, disregarding the wing, and to the two peaks in the 1:4 mixture (Lorentzian profiles were also attempted but were impossible to match to the ice peaks). The IDL simplex optimization routine was used to fit two Gaussian peaks simultaneously to the band in the 1:4 spectrum. Figure 3 shows that the bending mode in all other mixtures can be separated into these three peaks; the slight misfit on the blue wing in all mixtures is corrected for by an additional, small Gaussian centered at 1685 cm^{-1} with *FWHM* (Full Width at Half Maximum) 35 cm^{-1}. The position of the 1634 cm^{-1} peak is shifted with CO_2 concentration (2 to 8 cm^{-1} for the different mixtures), but the *FWHM*s of the Gaussians were always kept constant. The other peak positions were also kept constant. The positions, widths and intensities of the Gaussians used to fit the bending mode for each mixture are listed in Table 3.

The same bulk stretching peak apparent in the pure H_2O spectra is visible in all mixture spectra (Fig. 2, Col. b). As more CO_2 is mixed in, it acquires more of a double peak structure, but the total width of the band remains the same. In pure H_2O ice the peak at 3696 cm^{-1} (2.71 μm) attributed to the free/dangling OH stretch was not detected (Rowland et al. 1991). In contrast, Fig. 2, Col. a, shows that a free OH H_2O stretching band, centered around 3660 cm^{-1} (2.73 μm), attributed to the stretches of small H_2O clusters, is clearly present in all ice mixtures with CO_2 and is comparable in intensity to the bulk stretching band at high concentrations of CO_2. While the intensity of the H_2O libration mode clearly drops as more CO_2 is mixed in, it is difficult to tell whether the profile of the libration band is affected by the presence of CO_2, because of the overlap with the CO_2 bending mode.

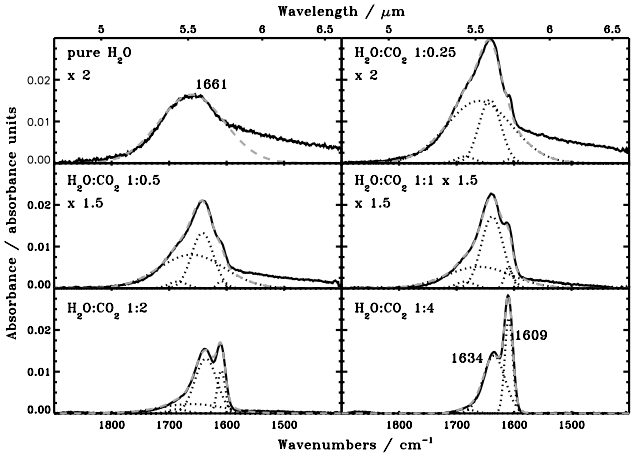

Fig. 3. The three Gaussian components present in the H_2O bending mode in mixtures with CO_2 disregarding the low frequency wing. In the *upper row*, first column the pure H_2O bending mode consists of a wing and a peak, where the peak was fitted with a Gaussian at 1661 cm^{-1}. In the *lower row*, second column, the H_2O bending mode in the 1:4 mixture can be separated into two narrow Gaussians at 1609 and 1634 cm^{-1}. The four other H_2O:CO_2 mixtures can be separated into these three components derived from the pure and 1:4 mixed ice. A small additional Gaussian centered at 1685 cm^{-1} accounts for some high frequency excess. The dotted lines indicate the individual Gaussian components and the dashed lines their sum.

Of all the H_2O bands, only the free OH stretching band grows in strength as the amount of CO_2 in the ice increases. The band strengths of all other H_2O ice bands drop with increased concentration of CO_2, as illustrated in Fig. 4, where all band strengths have been scaled to that of the H_2O stretch in

Table 4. The linear fit coefficients for the H_2O band strengths as functions of CO_2 concentrations in %, based on six experiments with 0 to 80% CO_2. The last two rows show the linear fit to the ratio between the bulk stretching and the bending mode.

		Linear coefficients		
Peak	Temperature	constant	linear coefficient	R^2
	[K]	[10^{-16} cm molecule^{-1}]	[10^{-19} cm molecule^{-1}]	
H_2O libration	15	0.32 ± 0.02	−3.2 ± 0.4	0.99
	45	0.42 ± 0.03	−2.7 ± 0.6	0.92
H_2O bend	15	0.14 ± 0.01	−0.5 ± 0.2	0.81
	45	0.17 ± 0.01	−0.6 ± 0.1	0.89
H_2O bulk stretch	15	2.1 ± 0.1	−22 ± 2	0.99
	45	2.8 ± 0.1	−21 ± 2	0.98
H_2O free OH stretch	15	0	1.62 ± 0.07	0.99
	45	0	1.40 ± 0.05	0.99
		constant	linear coefficient	R^2
H_2O bulk stretch/bend	15	16.7 ± 0.2	−0.160 ± 0.005	0.99
	45	17.0 ± 0.3	−0.101 ± 0.008	0.99

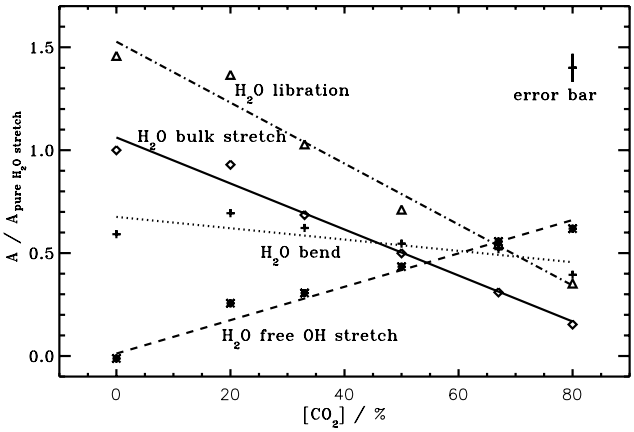

Fig. 4. The band strengths of the four main H_2O peaks in H_2O:CO_2 ice mixtures relative to that of the H_2O stretch in pure H_2O ice at 15 K. The band strengths of the libration, bend and free OH stretch modes have been multiplied by a factor of 10 to facilitate display. The estimated average error bar of the relative band strengths is shown in the upper right corner.

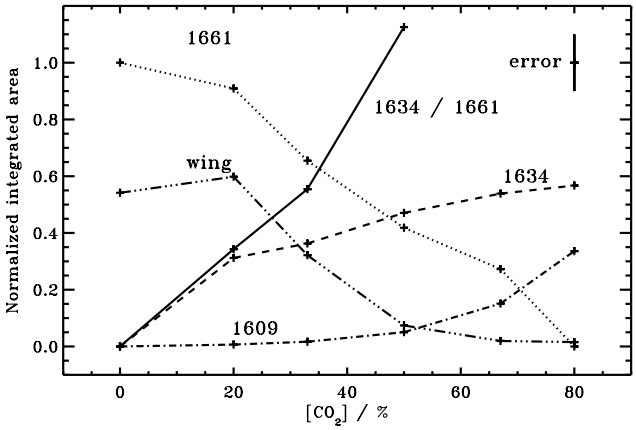

Fig. 5. The integrated area of the three Gaussian components present in the H_2O bending mode in mixtures with CO_2 and of the low frequency wing attributed to a librational overtone. The ratio between the 1634 and 1661 cm^{-1} peaks is plotted as well. The estimated error, shown as an error bar in the top right corner, is mainly due to the error in the total band strength and not to the Gaussian fit.

pure H_2O ice. The band strength of the bulk stretching band and the libration band are strongly dependent on the CO_2 concentration, while the intensity of the bending mode is less affected, whether the librational overtone is included or not, in calculating its integrated intensity. The relationship between the integrated peak intensities and CO_2 concentration is well described by linear models within this experimental domain and the data can be fitted with a typical squared correlation coefficient $R^2 = 0.98$ (Table 4). The correlations for the band strengths of the bending mode are considerably less, $R^2 = 0.81$ and 0.89 at 15 K and 45 K, respectively. This is due to the relatively small change in band strength with CO_2 concentration.

In addition, the relative strengths of the various components of the bending modes were calculated from the previously fitted Gaussians. The integrated areas relative to the pure H_2O bending mode are listed in Table 3 and plotted in Fig. 5 together with the area of the residual wing. The ratio between the 1661 and 1634 cm^{-1} peaks is plotted and its significance in astrophysical applications is discussed in Sect. 5.2. Table 3 also contains the total strength of the bending mode, excluding the wing. Due to the exclusion of the wing the drop in band strength with CO_2 concentration is smaller than in Fig. 4.

4.2. Temperature dependence

The profiles of all H_2O bands in the H_2O:CO_2 mixtures change systematically with temperature to become more similar to the bands of pure H_2O ice as the temperature is increased (Fig. 6). This is especially apparent for the bending mode, where the narrow bands lose intensity and the broad band, associated with pure H_2O ice, gains intensity as the temperature rises. This is also seen in Fig. 7 where the bending mode of the 1:0.5 mixture at 15, 45 and 75 K has been decomposed into the same components derived from the pure H_2O and 1:4 mixture at 15 K. As the temperature increases the shapes of the components remain the same, but the ratio between the thin components and the pure H_2O component decreases. The ratios for all mixtures at 15, 45 and 75 K are listed in Table 5.

The strengths of all H_2O bands increase with temperature, except for the free OH stretching band which decreases and disappears completely above 90 K. Figure 8 shows that the bulk stretching band increases monotonically in band strength, while the bending and libration bands display jumps and local minima. These jumps are most pronounced around the CO_2 desorption temperature (~90 K). As in the case of concentration dependency, the band strengths of the stretching and libration bands are more affected by temperature than the band strength

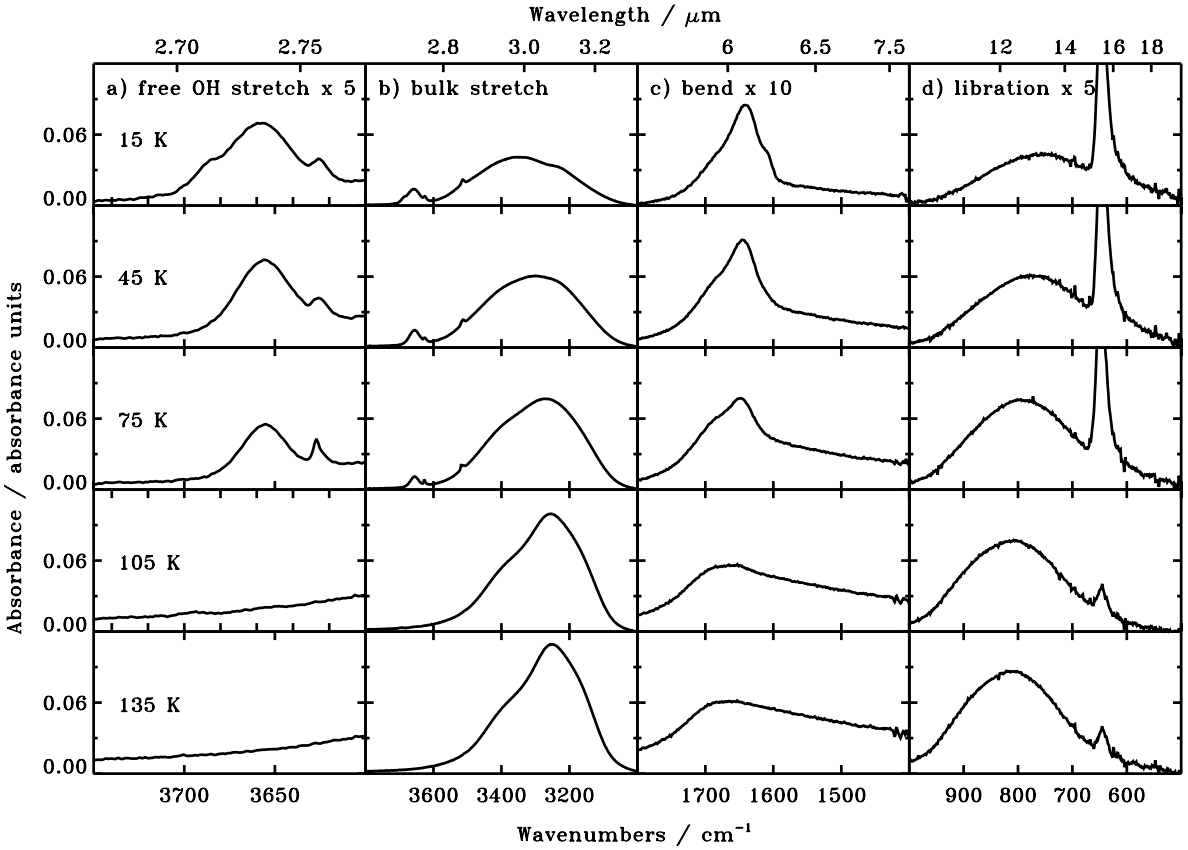

Fig. 6. Temperature dependence of the H_2O bands in a 1:0.5 H_2O:CO_2 mixture i.e. 67% H_2O and 33% CO_2. Spectra at 4000−400 cm^{-1} of the four main H_2O peaks in a 1:0.5 ice mixture with CO_2 at temperatures between 15 and 135 K. Each column contains one of the H_2O vibrational modes and each row one of the temperatures. **a)** An expanded view of the H_2O free OH stretch, **b)** the H_2O bulk and free-OH stretch, **c)** the H_2O bend and **d)** H_2O libration. The spectra of libration, bending and free OH stretch have been scaled, with a scaling factor indicated in the top row.

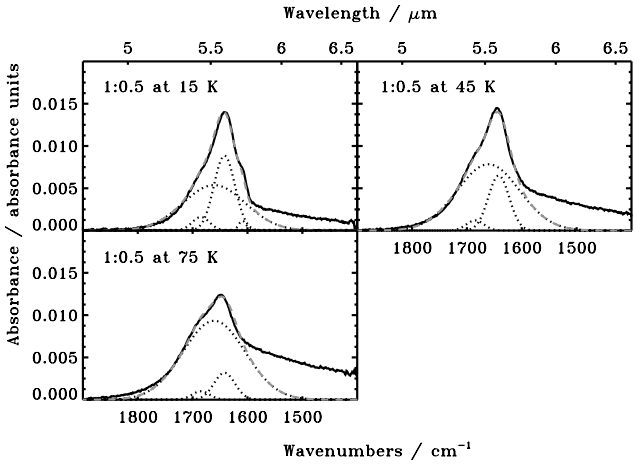

Fig. 7. The components present in the bending mode in the H_2O:CO_2 1:0.5 mixture at different temperatures. The same components that were derived in Fig. 4 have been used to fit the bending mode at 15, 45 and 75 K. These components are always present regardless of temperature, but the ratios between the different components changes, especially the ratio between the thin 1634 cm^{-1} and the pure H_2O 1661 cm^{-1} components decreases with temperature.

of the bending mode (including or excluding the libration overtone wing). Note that the profile of the bending mode is the most affected by both changes in temperature and CO_2 concentration, however.

Table 5. Ratios between the 1634 and 1661 cm^{-1} components for all mixtures at 15, 45 and 75 K.

	Ratio at given temperature		
Composition	15 K	45 K	75 K
pure H_2O	0	0	0
H_2O:CO_2 1:0.25	0.34	0.12	0.034
H_2O:CO_2 1:0.5	0.55	0.28	0.11
H_2O:CO_2 1:1	1.1	0.49	0.11
H_2O:CO_2 1:2	2.0	0.73	0.17
H_2O:CO_2 1:4	>10	1.6	0.31

Different bands are thus differently affected by an increasing temperature. In addition, the spectra of ice mixtures with higher CO_2 concentration are more affected by changes in temperature than those of ices with less CO_2; the influence of CO_2 concentration on the intensity ratio between the bulk stretching and the bending modes (including the libration overtone wing) is plotted in Fig. 9 for different temperatures between 15 and 135 K. In this plot the CO_2 concentration on the horizontal axis is the initial one. Above 90 K most of the CO_2 has desorbed, which changes the mixture composition. In addition, the ratio between the stretching mode and the sum of the bending mode components (excluding the wing) at 15 K is plotted for comparison. The parameters of the linear fit to the 15 and 45 K measured points are included in Table 4.

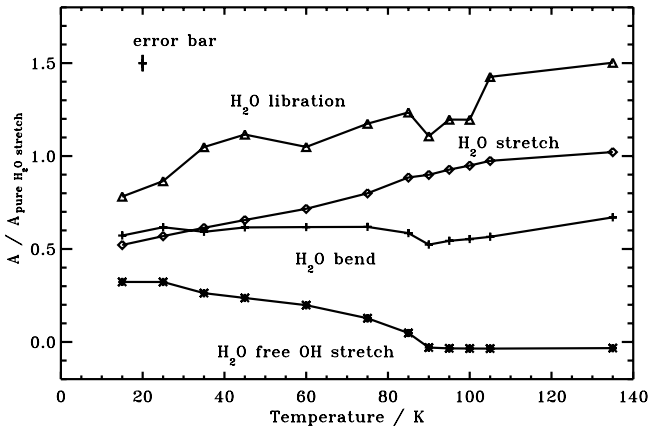

Fig. 8. The band strengths of the four main H_2O peaks in an initial 1:0.5 ice mixture with CO_2 at temperatures between 15 and 135 K relative to the band strength of the H_2O bulk stretch in pure H_2O ice at 15 K. The band strengths of the libration, bending and free-OH stretching mode have been scaled by 10 to facilitate viewing. The average error bar for the relative band strengths is shown in the upper left corner.

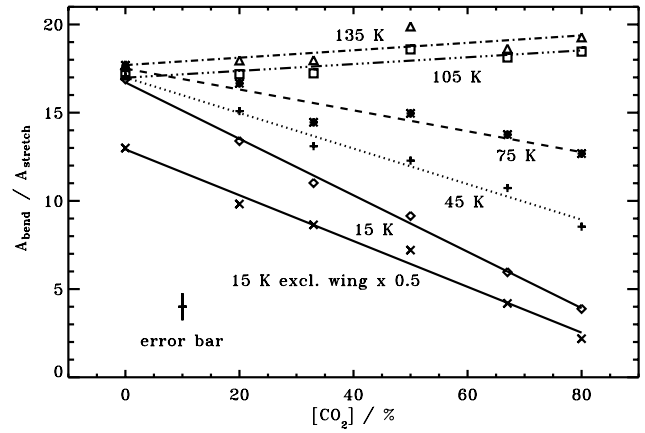

Fig. 9. The ratio between the H_2O bulk stretching and bending mode band strengths (including the libration overtone wing) for different temperatures in H_2O:CO_2 ice mixtures with increasing initial amounts of CO_2. The CO_2 concentration quoted is that of the initial ice mixture, while above 90 K most of the CO_2 has desorbed, changing the composition substantially. In addition the ratio between the stretching band and the bending mode components (excluding the libration overtone wing) is shown for 15 K (multiplied by 0.5 to facilitate viewing).

4.3. Dependence on additional parameters: deposition temperature and ice thickness

When the ice mixture (H_2O:CO_2 1:0.5) was deposited at 45 K instead of 15 K the profiles and band strengths of the ice bands did not change compared to those found when heating the 15 K mixture to 45 K. The profiles remain similar also at higher temperatures. As the ices are heated, the increase in H_2O bulk stretching band strength is significantly smaller for the ice deposited at 45 K compared to 15 K. In addition, 2−3 times as much CO_2 is retained in the H_2O ice at temperatures above the CO_2 desorption temperature of 85−90 K (Fig. 10).

Two control experiments with approximately three times more and three times less total ice thickness were run to test for changes in peak profiles and relative peak band strengths with thickness (not shown here). The relative peak band strengths did not change significantly for these experiments (i.e. less than the previously estimated experimental uncertainty of 10%). Nevertheless, the profile showed some thickness dependence, with the narrow peak in the bending mode being more pronounced for the experiments with less ice coverage.

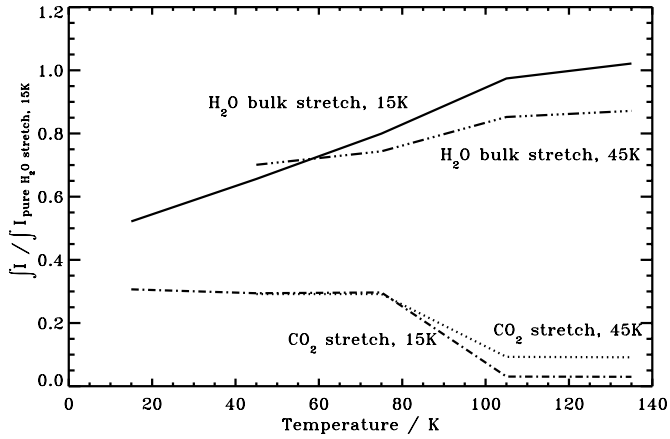

Fig. 10. The band strengths of the H_2O stretching mode deposited at 15 and 45 K in the 1:0.5 ices, respectively, relative to the band strength of the H_2O stretch in pure H_2O ice. The CO_2 stretching peak is plotted so the amount of CO_2 in the ice at different temperatures can be compared. The temperature labels given in the figure indicate the deposition temperature.

5. Discussion

5.1. Ice structure

The changes in the H_2O spectral features in H_2O:CO_2 ice mixtures, compared to the pure H_2O ice, demonstrate that the mixed-in CO_2 does affect the H_2O ice structure. The nature of the interaction between H_2O and CO_2 is not obvious. One possible scenario is that the CO_2 is spread out in the ice more or less uniformly and that the change in the H_2O peak intensities and profiles is due H_2O bonding with CO_2. A second option is that instead CO_2 forces the H_2O into small clusters, either in the gas-phase or upon arrival at the ice surface, since it is known from matrix isolated experiments and calculations that H_2O molecules form much stronger bonds with each other than with CO_2 (Tso & Lee 1985; Danten et al. 2005). The spectral changes would then originate from a different type of H_2O-H_2O interaction rather than H_2O bonding with CO_2.

The large decrease in band strength of the H_2O bulk stretching mode that is observed when CO_2 is mixed into the H_2O ice indicates that CO_2 destroys the bulk hydrogen-bond network, since the band strength of the stretching mode is weaker in small clusters compared to that in larger clusters and bulk ice (van Thiel et al. 1957). At the same time a new stretching peak appears at a higher frequency, i.e. more and more H_2O molecules are forced into a looser bound environment, which increases the intramolecular O-H bond strength, as the CO_2 concentration increases. The frequency of this band, ~2.7 μm, and its distinctness from the bulk stretching band make it possible to assign it to free OH stretches (Rowland et al. 1991), which in general occur both at surfaces of ice and in clusters. This agrees with more and more H_2O molecules isolated in clusters, and hence separated from the H_2O ice hydrogen-bond network as CO_2 is added, but not with a uniform arrangement with CO_2. Ehrenfreund et al. (1996) observed a similar band in different ice mixtures with 10% or less H_2O. They assigned it to overlapping peaks of H_2O monomers, dimers and small multimers consistent with our analysis. Similar conclusions were also drawn by van Thiel et al. (1957) based on their cluster experiments.

Simultaneously with the appearance of the free OH stretching band, the original broad band in the bending region drops in intensity and two narrow peaks appear. The narrowest of the two dominates at high CO_2 concentration and is at the approximate position of the H_2O dimer in argon at 1611 cm^{-1} (Ayers & Pullin 1976). However, the bending mode peaks of H_2O monomers, dimers and small clusters are not far apart and shift in position between different matrices (Tso & Lee 1985; van Thiel et al. 1957), thus rather than being due to only H_2O dimers it is more likely that this peak is produced by a mixture of monomer, dimer and small multimer peaks that are overlapping. The H_2O-CO_2 dimer has its main peak around 1598 cm^{-1} (Tso & Lee 1985) and is not visible, further indicating that increasing the amount of CO_2 lead to a majority of the H_2O clustered with themselves rather than bonded with CO_2.

Ehrenfreund et al. (1996) observed a similar bending mode to ours in a H_2O:N_2:O_2 1:5:5 mixture with a narrow peak at 1606 cm^{-1} and a broader feature at 1630 cm^{-1} assigned to H_2O monomers, dimers and small clusters and bulk H_2O ice, respectively. The fact that the same bending mode is acquired when H_2O is mixed with other small molecules corroborates our interpretation that the H_2O spectrum is dominated by the interaction between the H_2O molecules regardless of mixture composition, as long as the mixed-in molecules cannot form hydrogen bonds, or more generally, cannot form bonds with H_2O of comparable strength to the H_2O-H_2O bond. Matrix-isolation experiments show that e.g. H_2O-CO, another astrophysically relevant combination, forms hydrogen bonds, while H_2O-CO_2 does not (Tso & Lee 1985).

As the ice is heated the multimer peaks disappear quickly and all other peaks become more like those of pure H_2O. As the temperature increases the H_2O molecules can reorientate on their lattice points to a greater degree and form larger and larger hydrogen-bonded clusters and finally entire networks. This leads to a very small fraction of free OH bonds compared to those taking part in hydrogen bonds and hence only bulk vibrations show up in the spectra at high temperatures. Above 90 K the desorption of CO_2 further allows the hydrogen-bonds to reform. The temperature affects the H_2O molecules directly as well as indirectly through its effect on the mobility and final desorption of CO_2.

This scenario generally holds independent of whether the ice is deposited at 15 or 45 K. At both temperatures the deposited ice should be amorphous and porous, resulting in some CO_2 molecules becoming trapped in the H_2O ice as the ice is heated and the pores collapse. The H_2O peak profiles are similar at all temperatures, but it is clear that more CO_2 is trapped inside the H_2O ice when the ice is deposited at 45 K compared to 15 K. Figure 10 shows that the higher fraction of CO_2 coincides with a lower intensity of the H_2O bulk stretching band, indicating that the trapped CO_2 makes it more difficult for the hydrogen bond network to reform. It is not clear at this stage why the ice deposited at 45 K is capable, when heated, of trapping more CO_2 within the matrix, but it is most likely a kinetic effect, related to the compactness of the ice. The different ice structure then affects the relative rates at which pores collapse versus CO_2 diffusion and desorption during the heating process (Collings et al. 2003).

All experimental results are hence consistent with a model in which the H_2O molecules are present in the ice either as bulk H_2O ice or as small H_2O clusters. A higher CO_2 concentration forces more H_2O molecules into the cluster state. Since H_2O bulk ice spectra are different from H_2O cluster spectra, adding CO_2 to H_2O ice will significantly change the shapes and band strengths of the different H_2O peaks compared to pure H_2O ice. It is expected that other small molecules that cannot form H-bonds (or only very weak ones), e.g. O_2 and N_2, will affect H_2O similarly to CO_2, as indicated by the matrix experiments of Ehrenfreund et al. (1996). Our group is currently conducting a systematic series of experiment investigating the effects of N_2, O_2 and CO on H_2O spectral features in ice mixtures.

5.2. Astrophysical implications

Recent Spitzer observations of the CO_2 bending mode at 15 μm towards background stars indicate that 85% of the CO_2 column density is in a water-rich ice (Knez et al. 2005). To fit all H_2O and CO_2 features consistently, a combination of H_2O:CO_2 10:1 and 1:1 at 10 K (with the ratios of the two mixtures varying between 1:0 and 1.3:1 for different sources) was used to fit the CO_2 profile (Knez et al. 2005). It is hence not unlikely that some of the observed H_2O ice is in mixtures with close to equal concentrations of CO_2 and H_2O.

This study shows that CO_2 in H_2O:CO_2 ice mixtures affects the H_2O spectrum in three observable ways:

1. a free OH stretch peak appears around 2.73 μm;
2. the profile of the H_2O bending mode changes dramatically;
3. the H_2O stretching/bending mode strengths decrease linearly with CO_2 concentration.

When the free OH stretching region at 2.7 μm is observable the presence/absence of that band provides a stringent upper limit on the amount of CO_2 mixed into the H_2O ice. This region was covered by ISO for high mass YSOs and will be observed by Akari (ASTRO-F). It is not covered by Spitzer and cannot be observed from the ground. Hence it is not possible to use this region of the spectrum to constrain the CO_2 concentration in H_2O ice in most lines of sight.

Instead we will here use only spectral changes (2) and (3) to analyze the Spitzer and Keck spectra of the YSO B5:IRS1 after the silicate absorption has been removed (Boogert et al. 2004). We first compare the B5:IRS1 spectrum with laboratory spectra of pure H_2O, CO_2 ices at 15 K for reference. Then we deduce the maximum amount of H_2O that can be present in a H_2O:CO_2 1:1 mixture without a change in peak position for the H_2O bending mode and then we present the best fit achieved by simultaneously comparing the H_2O stretching and bending regions and the CO_2 bending mode to laboratory spectra of pure H_2O, CO_2 and H_2O:CO_2 mixtures at 15 K. An equally good fit is achieved using laboratory spectra acquired at 45 K, which is also shown. In addition, we show that the average H_2O:CO_2 mixture in the line of sight can be deduced by fitting the 6.0 μm region with the bending mode components in Fig. 3, while keeping the total H_2O bending mode integrated intensity consistent with that of the H_2O stretching mode. For all cases we also attempt to fit the excess in the H_2O bending region with HCOOH. The presence of HCOOH is strongly indicated by absorption features at 7.25 and 8.2 μm (8.2 μm not shown). HCOOH has also been suggested before as the most likely candidate for the blue wing of the 6.0 μm band (Schutte et al. 1996).

In the analysis of B5:IRS1 we did not take into account the effect of grain shapes on the absorption profiles. The effect on the H_2O bending profile should be small, however, due to that the imaginary part of the optical constant (k) for the H_2O bending profile is small. When k is small it induces (through Kramers-Kronig relation) only small fluctuations of n around the central peak wave number so that particle scattering will not

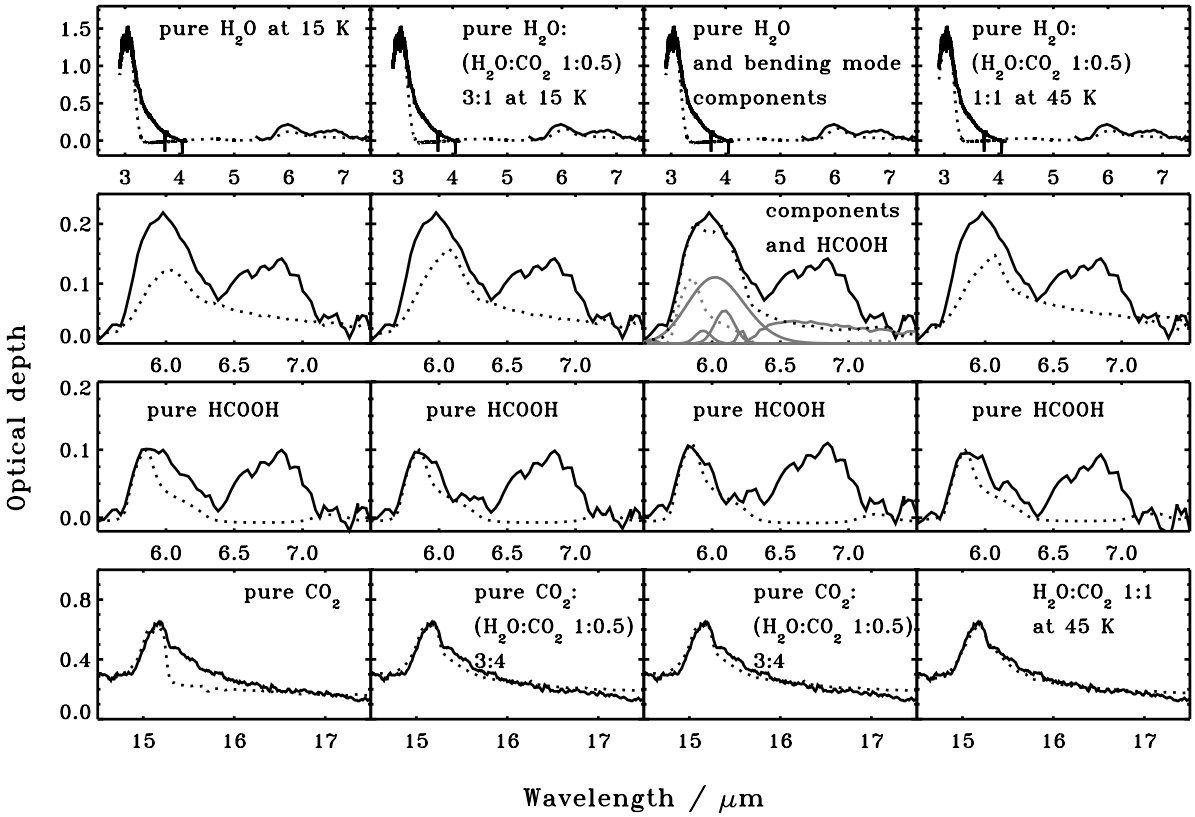

Fig. 11. Spectrum of the YSO B5 IRS1 (solid line) compared with laboratory spectra (dashed) of pure H_2O and CO_2 at 15 K (*first column*), a combination of pure H_2O and the H_2O:CO_2 1:0.5 ice mixture at 15 K (*second column*) and 45 K (*fourth column*) and the derived bending mode components (*third column*). The silicate feature has been subtracted from the B5:IRS1 spectrum in all plots. In the upper row the spectrum has been fitted with respect to the 3 μm H_2O stretching band. The effect on the H_2O bending mode region is shown in the second row. In the third row the H_2O (mixture) spectra have been subtracted from the star spectrum and the residual is compared with a pure HCOOH spectrum at 15 K. The last row shows the fit to the CO_2 bending mode using the ice mixture derived from the H_2O modes. The CO_2 peak has been shifted in the laboratory spectra to account for the shift in position between $C^{16}O_2$ and $C^{18}O_2$ used in this study. In the fourth column the spectrum of pure HCOOH was fitted together with the bending mode components to the 6.0 μm band, to achieve an optimal fit while also being consistent with the band strength of the H_2O stretching mode. The individual components are plotted with a gray line.

induce a significant change in band shape compared to transmission spectra.

In Fig. 11 the laboratory spectrum of pure H_2O is scaled to the 3.0 μm stretching band (upper row, first column). The fit in the bending mode region is shown in the second row and the spectrum after subtraction of the pure H_2O spectrum in the third row. A pure HCOOH spectrum was then scaled to the residual. The lower row shows the fit of the CO_2 bending mode when only a pure CO_2 spectrum is used. It is found that the fit between the pure laboratory ice spectrum and observed spectrum is poor. We subsequently tested the maximum amount of H_2O that can be mixed in the 1:1 mixture with CO_2 without visibly changing the H_2O bending mode profile. If 6% of the total H_2O column density is in a 1:1 mixture there is a clear change in peak position of the bending mode so 5% was set as an upper limit.

In the second column a combination of pure H_2O and the H_2O:CO_2 1:0.5 mixture at 15 K was used to fit the H_2O stretching and bending regions simultaneously. A good fit is also possible using the H_2O:CO_2 1:1 and 1:0.25 mixture. The best fit is achieved using 3 parts pure H_2O ice and 1 part 1:0.5 mixture. The pure/mixture combination results in a smaller residual in the H_2O bending region when subtracted from the B5:IRS1 spectrum, compared to when only a pure H_2O spectrum is used. In addition, the fit with the spectrum of HCOOH to this residual is better. The same 1:0.5 ice mixture, together with pure CO_2, is also used to fit the CO_2 15.2 μm bending mode. Approximately 50% of the CO_2 is found to be in a H_2O rich ice for the best fit. A combination of pure and 1:0.25 mixture also results in a good fit for the CO_2 bending mode, but a combination of pure ice and the 1:1 mixture. Hence fitting the H_2O and CO_2 ice modes simultaneously effectively constrains both the abundances and different environments of both H_2O and CO_2 ice.

The third column shows the best fit to the 6.0 μm region using the H_2O bending mode components derived previously and pure HCOOH. This method of estimating the composition of water rich ice has the advantage that no mix and matching with different laboratory spectra is needed and the uncertainty is easier to estimate. The three components were varied independently, but the wing residual was scaled to the pure H_2O component. The ratio between the broad pure H_2O peak at 6.02 μm (1661 cm^{-1}) and the 6.09 μm (1642 cm^{-1}) peak was used to constrain the amount of CO_2 present by comparing this ratio to Fig. 5. The total H_2O bending mode integrated intensity was constrained by the ratio between the stretching and bending mode band strengths including the wing (Table 4) and the ratio between the broad pure H_2O component and the narrow H_2O cluster bending component (Table 5). The latter comparison constrains the amount of H_2O mixed with CO_2, which must be fed back into the ratio between the stretching and the total bending mode strength to calculate a correct column density.

Table 6. Column densities derived from the different fits to the B5:IRS1 spectra.

Composition	$N(H_2O_{total})^a$ (cm^{-2})	$N(H_2O_{pure})$ / $N(H_2O_{total})$	$N(H_2O_{mixed})$ / $N(H_2O_{total})$	$N(CO_{2\ total})$ / $N(H_2O_{total})$	$N(CO_{2\ pure})$ / $N(H_2O_{total})$	$N(CO_{2\ mixed})$ / $N(H_2O_{total})$
pure H_2O at 15 K[b]	2.1×10^{18}	1	0	0.32	0.32	0
H_2O:(H_2O:CO_2 1:0.5) =3:1 at 15 K[c]	2.3×10^{18}	0.75	0.25	0.23	0.10	0.13
H_2O:CO_2 ~90:10[d] assuming 15 K	2.2×10^{18}	0	1	–	–	0.08−0.14
H_2O:(H_2O:CO_2 1:0.5) =1:1 at 45 K[e]	1.7×10^{18}	0.5	0.5	0.20	0	0.20

[a] From H_2O stretching mode; [b] first column in Fig. 11; [c] second column in Fig. 11, preferred fit at 15 K; [d] third column in Fig. 11; [e] fourth column in Fig. 11, preferred fit at 45 K.

A good fit was achieved for average H_2O:CO_2 mixtures 92:8 to 86:14, which is consistent with the derived composition from the best fit in the second column. When higher resolution spectra of this region will be available, it should be possible to analyze all the different components of the H_2O bending mode as demonstrated in the laboratory spectrum (Fig. 3). This will further constrain the mixture composition from the ratio between the two narrow bending peaks apparent in all mixture spectra. In the current spectrum the ratio between the two narrow peaks only puts an upper limit of 1:1 on the dominant H_2O:CO_2 mixture in the line of sight. The column densities derived from the fit of laboratory spectra and bending mode components are shown in Table 6.

All the fits above were done with spectra at 15 K. If the observed ice is at a higher temperature, the same amount of CO_2 mixed into the ice will result in a H_2O bending mode profile that is less different from pure H_2O ice (Fig. 6). The best fit at 45 K has an average mixture of H_2O:CO_2 ~ 1:0.23 (with 50% of the H_2O ice in a 1:0.5 mixture and 50% pure H_2O) and then no additional pure CO_2 is necessary to fit the CO_2 bending mode. A similar result is achieved when fitting the H_2O bending mode components and calculating the composition using the values of the component ratios for 45 K instead of 15 K in Table 5. More generally the ratio of the components constrains a region in the ice mixture-temperature space (initial mixture if the temperature is above 90 K) rather than determining an exact mixture composition. The fit to B5:IRS1 resulted in a ratio of the 1634 to 1661 cm^{-1} components of 0.15. According to Table 5 this means that the temperature:composition is bound by 15 K:11 ± 3%, 45 K:23 ± 3% and 75 K:39 ± 5% CO_2 relative to the H_2O ice abundance. Using the components to fit the bending region rather than spectra is advantageous if the temperature is unknown, since the ratio between the components sets bounds on the temperature and composition simultaneously and fully reveals the uncertainties involved. In most sources it is possible to independently constrain the temperature, however. For B5:IRS1 Boogert et al. (2004) have concluded that the bulk of the ice must be colder than 50 K. For these temperatures the ratio of the bending mode components results in an average H_2O:CO_2 mixture of 11 to 23% CO_2 with respect to the H_2O ice. This can be further refined by more detailed radiative transfer modeling of the dust temperature in the source by fitting the spectral energy distribution. In contrast the total abundances of H_2O and CO_2 are only weakly dependent on temperature and can be determined within 15% uncertainty.

Note that the strengths of the stretching and libration bands are affected by CO_2, which needs to be taken into account when deducing the H_2O column density from the optical depths of the H_2O bands if a considerable amount of the H_2O is in mixtures with CO_2. In the example shown here the drop in band strength of the stretching band is only ~5% compared to the pure H_2O ice (Table 6). In the case where ~50% of the H_2O ice is in a 1:1 mixture with CO_2, as has been deduced for some background stars by Knez et al. (2005), the band strength of the H_2O stretching mode would drop by as much as ~25% compared to pure H_2O ice and the inferred H_2O column density would be ~33% higher.

Whether the results presented here can explain the ratio between the H_2O stretching and bending modes in all astrophysical sources has to be determined for each source individually because of the drastic change in the bending mode profile that accompanies the drop in ratio as the concentration of CO_2 is increased. In the case of B5:IRS1 the H_2O and CO_2 band shapes and intensities are well described by 50% of the CO_2 and 25% of the H_2O ice in a H_2O:CO_2 1:0.5 ice mixture at 15 K and by 100% of the CO_2 and 50% of the H_2O ice in a H_2O:CO_2 1:0.5 ice mixture at 45 K. These ratios in turn can provide interesting constraints on the H_2O and CO_2 formation routes.

6. Conclusions

1. The H_2O band profiles and strengths in astrophysically plausible mixtures with CO_2 are significantly different compared to pure H_2O ice. The changes in H_2O band profiles with CO_2 are greatest for the H_2O bending mode, while the stretching band displays more subtle changes.
2. The band strengths of all major H_2O bands depend linearly on CO_2 in the investigated domain of 20% to 80% of CO_2 in the ice mixture. The band strength ratio between the H_2O bulk stretching and bending modes is also linearly dependent on CO_2 concentration in astrophysically relevant H_2O:CO_2 mixtures such that a H_2O:CO_2 1:1 mixture has a ratio of half that of pure H_2O.
3. The H_2O bending mode in H_2O:CO_2 mixtures can be separated into three components due to pure H_2O ice, large H_2O and small H_2O clusters, respectively. In addition, a librational overtone overlaps with the bending mode.
4. The H_2O bending profile is visibly affected by as little as 6% H_2O in a H_2O:CO_2 1:1 mixture. The composition of the H_2O rich ice is hence crucial to identify other species contributing to the 6 μm band.
5. A free OH stretching band appears with CO_2 concentration which can be used to put strict upper limits on CO_2 mixed with H_2O whenever the 2.7 μm region is observed.
6. If the ice temperature can be estimated independently, the total amount of CO_2 and H_2O as well as the amount of CO_2 mixed with the H_2O ice can be constrained by fitting the

appropriate laboratory mixture spectra consistently to the H_2O and CO_2 bands.

7. The average H_2O:CO_2 ice mixture in any line of sight can be efficiently deduced by fitting the H_2O bending mode with components corresponding to pure and CO_2 rich ice. Especially if the ice temperature is uncertain, fitting the H_2O bending mode components to the bending mode region together with HCOOH, will effectively constrain the composition and temperature simultaneously.
8. The deduction of mixture composition is substantially dependent on the assumed dust temperature. The determination of total column densities of H_2O and CO_2 are only weakly dependent on the assumed dust temperature, however.

Acknowledgements. We thank Claudia Knez for initiating the discussion that prompted this study. We also thank the referee, Bernard Schmitt, for helpful comments on the manuscript. Funding was provided by NOVA, The Netherlands Research School for Astronomy, a grant from the European Early Stage Training Network ("EARA" MEST-CT-2004-504604) and a NWO Spinoza grant.

References

Ayers, G. P., & Pullin, A. D. E. 1976, Spectrochim. Acta, 32A, 1629
Bergin, E. A., Melnick, G. J., Gerakines, P. A., Neufeld, D. A., & Whittet, D. C. B. 2005, ApJ, 627, L33
Bernstein, M. P., Cruikshank, D. P., & Sandford, S. A. 2005, Icarus, 179, 527
Boogert, A. C. A., Tielens, A. G. G. M., Ceccarelli, C., et al. 2000, A&A, 360, 683
Boogert, A. C. A., Pontoppidan, K. M., Lahuis, F., et al. 2004, ApJS, 154, 359
Collings, M. P., Dever, J. W., Fraser, H. J., McCoustra, M. R. S., & Williams, D. A. 2003, ApJ, 583, 1058
Danten, Y., Tassaing, T., & Besnard, M. 2005, J. Phys. Chem. A, 109, 3250
Devlin, J. P., Sadlej, J., & Buch, V. 2001, J. Phys. Chem. A, 105, 974
Ehrenfreund, P., Gerakines, P. A., Schutte, W. A., van Hemert, M. C., & van Dishoeck, E. F. 1996, A&A, 312, 263
Gerakines, P. A., Schutte, W. A., Greenberg, J. M., & van Dishoeck, E. F. 1995, A&A, 296, 810
Gerakines, P. A., Whittet, D. C. B., Ehrenfreund, P., et al. 1999, ApJ, 522, 357
Gerakines, P. A., Bray, J. J., Davis, A., & Richey, C. R. 2005, ApJ, 620, 1140
Gibb, E. L., & Whittet, D. C. B. 2002, ApJ, 566, L113
Gibb, E. L., Whittet, D. C. B., Boogert, A. C. A., & Tielens, A. G. G. M. 2004, ApJS, 151, 35
Hagen, W., Tielens, A. G. G. M., & Greenberg, J. M. 1983, A&AS, 51, 389
Hudgins, D. M., Sandford, S. A., Allamandola, L. J., & Tielens, A. G. G. M. 1993, ApJS, 86, 713
Keane, J. V., Boonman, A. M. S., Tielens, A. G. G. M., & van Dishoeck, E. F. 2001, A&A, 376, L5
Knez, C., Boogert, A. C. A., Pontoppidan, K. M., et al. 2005, ApJ, 635, L145
Murakawa, K., Tamura, M., & Nagata, T. 2000, ApJS, 128, 603
Nummelin, A., Whittet, D. C. B., Gibb, E. L., Gerakines, P. A., & Chiar, J. E. 2001, ApJ, 558, 185
Palumbo, M. E., & Baratta, G. A. 2000, A&A, 361, 298
Pontoppidan, K. M., Dullemond, C. P., van Dishoeck, E. F., et al. 2005, ApJ, 622, 463
Rowland, B., Fisher, M., & Devlin, J. P. 1991, J. Phys. Chem., 95, 1378
Sandford, S. A., & Allamandola, L. J. 1990, ApJ, 355, 357
Schmitt, B., Greenberg, J. M., & Grim, R. J. A. 1989, ApJ, 340, L33
Schutte, W. A., Tielens, A. G. G. M., Whittet, D. C. B., et al. 1996, A&A, 315, L333
Tanaka, M., Sato, S., Nagata, T., & Yamamoto, T. 1990, ApJ, 352, 724
Tso, T., & Lee, E. K. C. 1985, J. Phys. Chem., 89, 1612
van Thiel, M., Becker, E. D., & Pimentel, G. C. 1957, J. Chem. Phys., 27, 486
Whittet, D. C. B., Gerakines, P. A., Tielens, A. G. G. M., et al. 1998, ApJ, 498, L159
Willner, S. P., Gillett, F. C., Herter, T. L., et al. 1982, ApJ, 253, 174